Nanoscale Advances

ROYAL SOCIETY OF CHEMISTRY

PAPER

View Article Online
View Journal | View Issue

Cite this: *Nanoscale Adv.*, 2024, **6**, 3948

A multidentate copper complex on magnetic biochar nanoparticles as a practical and recoverable nanocatalyst for the selective synthesis of tetrazole derivatives†

Marwan Majeed Maseer,[a] Tavan Kikhavani*[a] and Bahman Tahmasbi *[b]

Waste recycling, novel and easy methods of recycling catalysts, use of green solvents, use of selective catalysts and preventing the production of by-products are the most important principles of green chemistry and modern technology. Therefore, in this work, biochar nanoparticles (B-NPs) were synthesized by the pyrolysis of chicken manure as a novel method for waste recycling. Subsequently, the B-NPs were magnetized by Fe(0) nanoparticles to improve the easy recovery of biochar. Then, the surface of biochar magnetic nanoparticles (FeB-MNPs) was modified by (3-chloropropyl)trimethoxysilane (3Cl-PTMS). Finally, a multidentate copper complex of 2,2′-(propane-1,3-diylbis(oxy))dianiline (P.bis(OA)) was immobilized on the surface of modified FeB-MNPs, which was labeled as Cu-P.bis(OA)@FeB-MNPs. Cu-P.bis(OA)@FeB-MNPs was investigated as a commercial, homoselective, practical, and recyclable nanocatalyst in the synthesis of 5-substituted-1*H*-tetrazole compounds through the [3 + 2] cycloaddition of sodium azide (NaN_3) and organo-nitriles in polyethylene glycol 400 (PEG-400) as a green solvent. Cu-P.bis(OA)@FeB-MNPs was characterized using wavelength dispersive X-ray (WDX) spectroscopy, scanning electron microscopy (SEM), thermogravimetric analysis (TGA), energy-dispersive X-ray spectroscopy (EDS), vibrating-sample magnetometer (VSM), atomic absorption spectroscopy (AAS) and N_2 adsorption–desorption (Brunauer–Emmett–Teller (BET) method) techniques. Cu-P.bis(OA)@FeB-MNPs was recovered and reused for several runs in the synthesis of tetrazoles.

Received 4th April 2024
Accepted 10th June 2024

DOI: 10.1039/d4na00284a

rsc.li/nanoscale-advances

1. Introduction

Chemical sciences is one of the most important fields for development in the world, which provides many applications in the fields of medicine and various industries. However, unfortunately, waste chemical materials have also been introduced into the environment during the growth of chemical science. Therefore, principles of green chemistry were introduced, which minimize the environmental damage from chemical industries and laboratories. One of the principles of green chemistry is the use of recyclable catalysts.[1–5] Acids, bases, and transition metals or metal complexes are among the most well-known types of catalysts. In general, catalysis systems are divided into two categories: homogeneous catalysis systems and heterogeneous catalysis systems.[6] Homogeneous catalysts are known to exhibit several properties such as high performance, selectivity, instability, difficult to recover, and time-consuming product purification.[7,8] On the other side, heterogeneous catalysts are known to exhibit different properties such as good recoverability, high stability, low efficiency, and selectivity.[7,8] Recently, nanocatalysts have emerged as a new category of catalyst systems that act as the bridge between homogeneous and heterogeneous catalysts and have advantages over both homogeneous and heterogeneous catalysts.[6,8–12] Because decreasing the particle size provides a high surface area, the catalytic activity and selectivity are increased (*e.g.*, homogeneous catalysts). In addition, nanomaterials have high stability and are heterogeneous in nature, enabling them to be easily recovered and reused like heterogeneous catalysts. In this context, various nanoparticles such as boehmite,[13–15] mesoporous silica materials,[16–18] graphene oxide,[19–21] MOF compounds,[22–31] carbon nanostructures,[32,33] polymers,[34] biochar,[35,36] and magnetic particles[37] have been reported as catalysts or catalyst supports. However, most of these materials are synthesized from mineral and non-renewable chemical compounds, which are against the principles of green and modern chemistry. Raw materials for biochar production include wood chips, tree bark, plant residues, animal manure, and organic wastes.[38–40] As is known, the use of renewable materials and waste recycling are other principles of green

[a]*Department of Chemical Engineering, Faculty of Engineering, Ilam University, Ilam, Iran. E-mail: t.kikhavandi@ilam.ac.ir*

[b]*Department of Chemistry, Faculty of Science, Ilam University, P. O. Box 69315516, Ilam, Iran. E-mail: b.tahmasbi@ilam.ac.ir; bah.tahmasbi@gmail.com*

† Electronic supplementary information (ESI) available. See DOI: https://doi.org/10.1039/d4na00284a

chemistry.[41,42] The synthesis of biochar nanoparticles from natural and renewable sources is very important in expanding its application. Considering the increasing importance of the catalysts in various industries and laboratories, the introduction of the catalysts (*e.g.* biochar) made from renewable sources is a necessity for the future. On the other hand, the increase in the population has led to the accumulation of a large amount of waste, which has become a challenge for the planet and the future of mankind. Therefore, recently, the technology of recycling waste and turning waste into valuable materials is of special interest, so that one of the principles of green chemistry is dedicated to this challenge. Considering that biochar synthesis is a novel method for waste recycling, it doubles the importance of expanding the use of biochar. Therefore, in this work, biochar nanoparticles were synthesized by the pyrolysis of chicken manure as a method for recycling agricultural waste. In fact, biochar is stable carbon black, and its surface is covered by C=O, COOH, and OH groups that provide a modifiable surface for the immobilization of catalyst species.[43–47] Despite the special advantages of biochar, it has rarely been reported as a catalyst or catalyst support. Despite the unique advantages of biochar, the separation and recycling of biochar nanoparticles require time-consuming and difficult methods such as centrifugation and filtration. This limitation can be overcome by biochar magnetic nanocomposites as a new and ideal methodology, which can be easily separated by an external magnet.[48–51] For example, in 2024 biochar was magnetized by magnetic Fe_3O_4 nanoparticles[36] and magnetic Ni nanoparticles.[48] But, biochar, and Fe(0) particles – with high surface area and stability – have rarely been used for the magnetization of materials.[52] Therefore, in this work, a complex of copper on magnetic biochar nanoparticles (Cu-P.bis(OA)@FeB-MNPs) was prepared as a new recyclable nanocatalyst for the homoselective synthesis of 5-substituted-1*H*-tetrazole compounds through [3 + 2] the cycloaddition of NaN_3 and organo-nitriles in PEG-400 as a green solvent. This is the first report on a copper complex of 2,2′-(propane-1,3-diylbis(oxy))dianiline on magnetic biochar nanoparticles and its introduction as a green catalyst in the synthesis of organic compounds.

2. Experimental

2.1. Preparation of biochar magnetic nanoparticles (FeB-MNPs)

Biochar nanoparticles were formed by simple pyrolysis of chicken manure. In this context, 500 g of dried chicken manure was heated at 400 °C as the pyrolysis temperature for 1 h under N_2 sweeping. At the end of pyrolysis, the heating was stopped and the Chinese crucibles were cooled with N_2 sweep. The resulting black solid was biochar. Then, 4.5 g of the synthesized biochar was mixed with $FeCl_2 \cdot 4H_2O$ (5.34 g) in ethanol (25 mL) and H_2O (5 mL), and then, it was stirred at room temperature for 15 min. Then, $NaBH_4$ (2.5 g in 70 mL of H_2O) as a reduction agent was injected into the mixture dropwise within 20 min. The obtained mixture was stirred at room temperature for 15 min. The magnetic powder (biochar magnetic nanoparticles) was filtered by magnetic decantation, washed with ethanol and dried for 6 h at 90 °C.[52]

2.2. Modification of FeB-MNPs with (3-chloropropyl) trimethoxysilane (3Cl-PTMS)

FeB-MNPs (1 g) were dispersed in *n*-hexane (25 mL) for 30 min by an ultrasonic bath. Then, (3-chloropropyl)trimethoxysilane (1.5 mL) was injected into it and was allowed to stir for 24 h under reflux conditions. After 24 h, the mixture was cooled to room temperature, and the modified FeB-MNPs (3Cl-PTMS@FeB-MNPs) were separated by magnetic decantation and washed with ethanol. The modified FeB-MNPs were dried at 60 °C (Scheme 1).

2.3. Functionalization of FeB-MNPs with P.bis(OA) (P.bis(OA)@FeB-MNPs)

FeB-MNPs (1 g) was mixed with P.bis(OA) (1 mmol) and triethylamine (8 mmol) in toluene (10 mL) and it was dispersed for

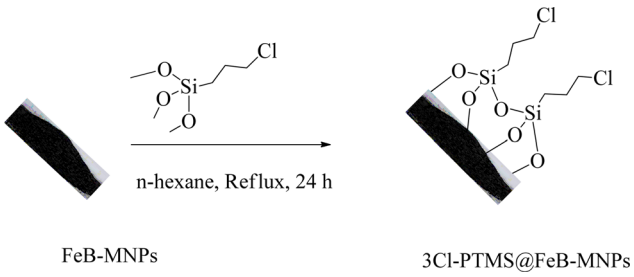

Scheme 1 Synthesis of 3Cl-PTMS@FeB-MNPs.

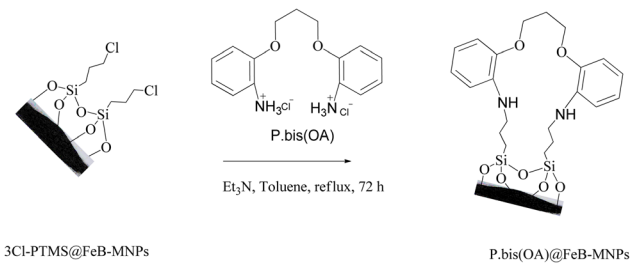

Scheme 2 Synthesis of functionalized FeB-MNPs with P.bis(OA) (P.bis(OA)@FeB-MNPs).

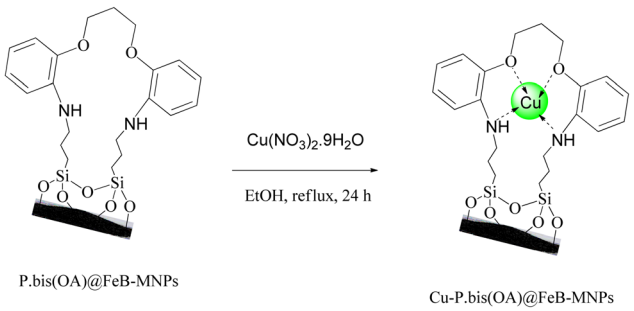

Scheme 3 Synthesis of Cu-P.bis(OA)@FeB-MNPs.

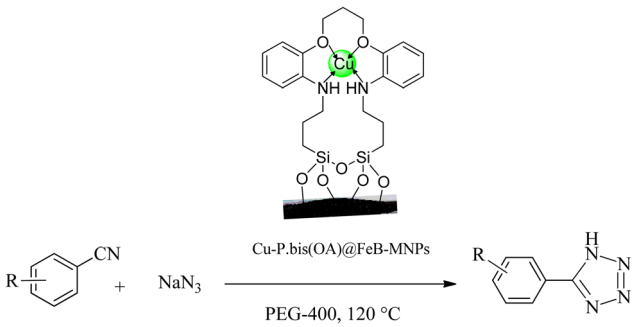

Scheme 4 Synthesis of tetrazoles in the presence of Cu-P.bis(OA)@FeB-MNPs.

25 min in an ultrasonic bath. Then, the mixture was stirred for 72 h under reflux conditions. The mixture was allowed to cool to room temperature. After that, the functionalized FeB-MNPs with P.bis(OA) (P.bis(OA)@FeB-MNPs) were filtered by magnetic decantation and then washed 5 times with dimethyl sulfoxide (DMSO) and ethanol. The obtained P.bis(OA)@FeB-MNPs were dried at room temperature (Scheme 2).

2.4. Synthesis of Cu-P.bis(OA)@FeB-MNPs

P.bis(OA)@FeB-MNPs (1 g) was mixed with $Cu(NO_3)_2 \cdot 9H_2O$ (2 mmol) in 25 mL of ethanol. The mixture was stirred under reflux conditions for 24 h. After that, the mixture was cooled. Then, the prepared final catalyst (Cu-P.bis(OA)@FeB-MNPs) was separated by magnetic decantation and washed several times with water and ethanol to remove excess copper from the mixture. Finally, Cu-P.bis(OA)@FeB-MNPs were kept at a temperature of 50 °C, which was dried (Scheme 3).

2.5. Synthesis of tetrazoles catalyzed by Cu-P.bis(OA)@FeB-MNPs

The catalytic application of Cu-P.bis(OA)@FeB-MNPs was investigated in the synthesis of tetrazoles through a ring addition reaction of nitrile and sodium azide (Scheme 4). A mixture of nitrile (1 mmol), sodium azide (1.4 mmol) in PEG-400 solvent, and 30 mg of Cu-P.bis(OA)@FeB-MNPs was stirred at a temperature of 120 °C. The reaction time was monitored by thin-layer chromatography (TLC) using UV wavelengths of 254 and 356 nm in acetone : *n*-hexane (8 : 2) tank solvent. After completion of the reaction, the reaction mixture was cooled and

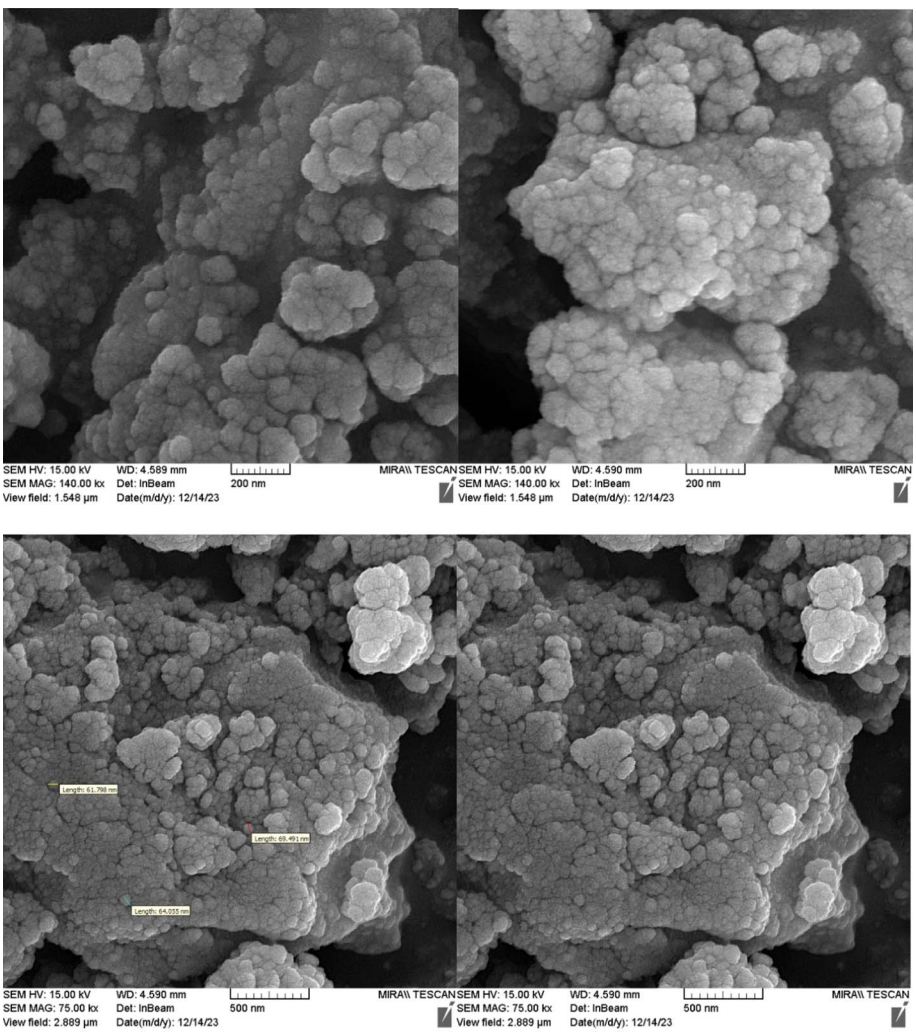

Fig. 1 SEM images of Cu-P.bis(OA)@FeB-MNPs.

diluted with ethyl acetate, distilled water, and HCl solution (4 N). Then, the Cu-P.bis(OA)@FeB-MNPs catalyst was isolated from the mixture and washed with ethyl acetate and HCl solution (4 N). After that, tetrazole products were extracted in ethyl acetate solvent. The organic phase was removed by evaporation to obtain 5-substituted 1*H*-tetrazoles.

2.6. NMR spectra of the tetrazoles

2-(1*H*-Tetrazol-5-yl)benzonitrile. ^{1}H NMR (250 MHz, DMSO): $\delta_H = 8.06$ (d, $J = 5.42$ Hz, 2H), 7.92 (t, $J = 7.05$ Hz, 1H), 7.76 (t, $J = 7.12$ Hz, 1H) ppm.

4-(1*H*-Tetrazol-5-yl)benzonitrile. ^{1}H NMR (250 MHz, DMSO): $\delta_H = 8.20$ (d, $J = 8.22$ Hz, 2H), 8.08 (d, $J = 4.95$ Hz, 2H) ppm.

5-(3-Nitrophenyl)-1*H*-tetrazole. ^{1}H NMR (250 MHz, DMSO): $\delta_H = 8.81$ (s, 1H), 8.42 (t, $J = 8.25$ Hz, 2H), 7.88 (t, $J = 7.62$ Hz, 1H) ppm.

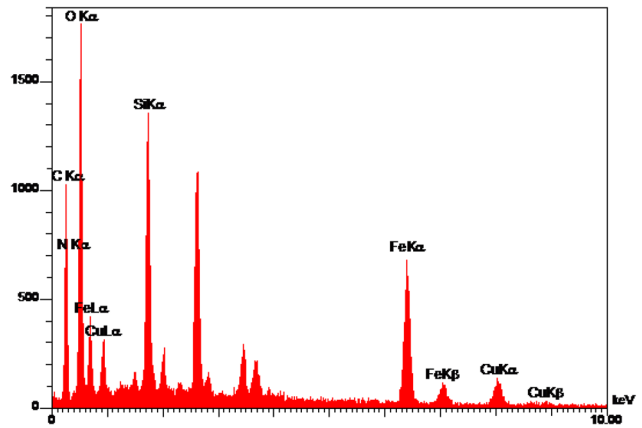

Fig. 2 The EDS diagram of Cu-P.bis(OA)@FeB-MNPs.

5-Phenyl-1*H*-tetrazole. ^{1}H NMR (250 MHz, DMSO): $\delta_H = 8.04$ (m, 2H), 7.59 (m, 3H) ppm.

5-(2-Chlorophenyl)-1*H*-tetrazole. ^{1}H NMR (250 MHz, DMSO): $\delta_H = 7.79$ (d, $J = 5.90$ Hz, 1H), 7.70 (d, $J = 6.35$ Hz, 1H), 7.58 (m, 2H) ppm.

5-(4-Chlorophenyl)-1*H*-tetrazole. ^{1}H NMR (250 MHz, DMSO): $\delta_H = 8.03$ (d, $J = 6.65$ Hz, 2H), 7.67 (d, $J = 6.75$ Hz, 2H) ppm.

3. Results and discussion

In this work, a heterogeneous catalyst of copper complex was immobilized on FeB-MNPs. Then, this nanocatalyst was characterized by WDX, SEM, TGA, EDS, VSM, AAS, and BET techniques. Then, its catalytic performance was investigated in the homoselective synthesis of tetrazoles.

3.1. Particle size and morphological identification of Cu-P.bis(OA)@FeB-MNPs by SEM

Fig. 1 shows the SEM images of Cu-P.bis(OA)@FeB-MNPs. As can be seen in SEM images, Cu-P.bis(OA)@FeB-MNPs have similar spherical shapes and uniform diameters of less than 70 nm. Also, the observed agglomeration of its particles in the SEM images is due to the magnetic nature of these nanoparticles.

3.2. Qualitative studying of the elements content of Cu-P.bis(OA)@FeB-MNPs

EDS analysis of Cu-P.bis(OA)@FeB-MNPs is shown in Fig. 2. Magnetic biochar nanoparticles are composed of C, O, and Fe, and after their surface modification, it is functionalized with (3-chloropropyl)trimethoxysilane. Also, the 2,2′-(propane-1,3-diylbis(oxy))dianiline ligand is composed of N, O, and C, which is complexed with Cu metal. Therefore, the composition

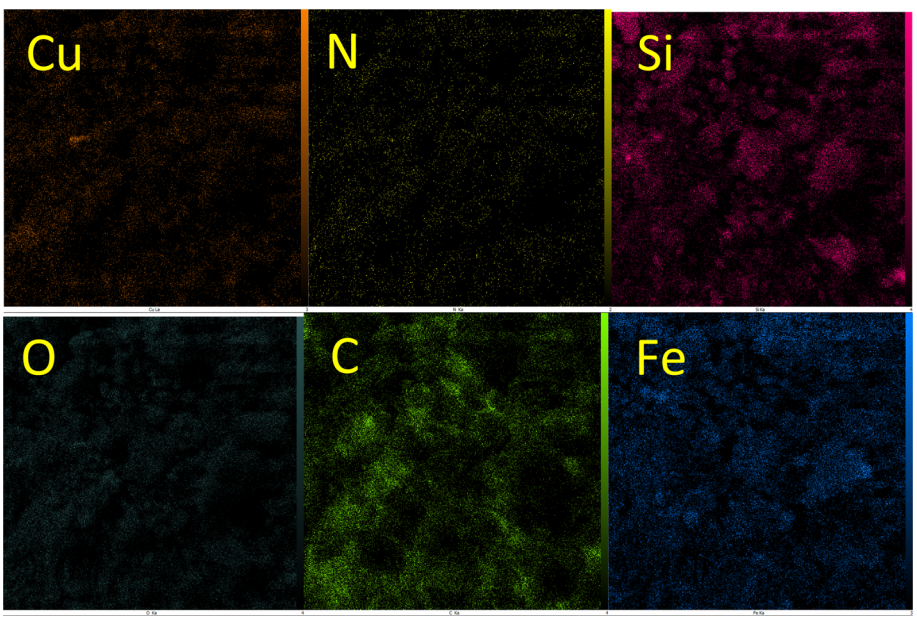

Fig. 3 WDX images of Cu-P.bis(OA)@FeB-MNPs.

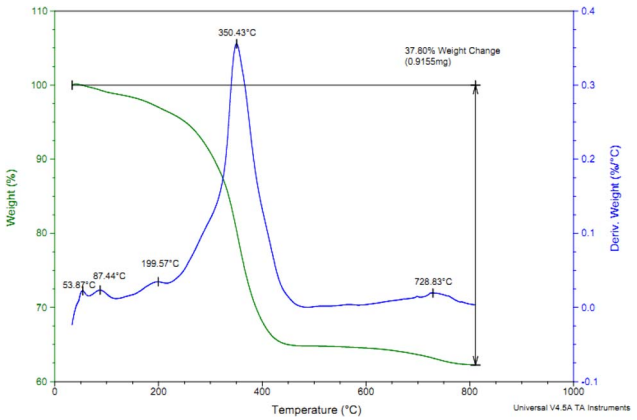

Fig. 4 TGA/DTG diagrams for Cu-P.bis(OA)@FeB-MNPs.

of Cu-P.bis(OA)@FeB-MNPs must include all these elements. As it is clear in the EDS analysis, all these elements are present in the composition of this catalyst, which indicates the successful synthesis of Cu-P.bis(OA)@FeB-MNPs. All C, O, Si, Cu, and N elements were observed in the catalyst structure. These evidences show that the synthesis of this catalyst was done successfully. As indicated in the EDS diagram, Cu-P.bis(OA) @FeB-MNPs are formed from C, N, O, Si, Fe, and Cu elements. The presence of Si element in this catalyst confirmed that FeB-MNPs were successfully modified by Cl-PTMS. Considering that silicon element was not present in the structure of the magnetic biochar nanoparticles and the elemental composition difference between FeB-MNPs and 3Cl-PTMS@FeB-MNPs is the presence or absence of silicon, therefore, the presence of silicon element in the elemental

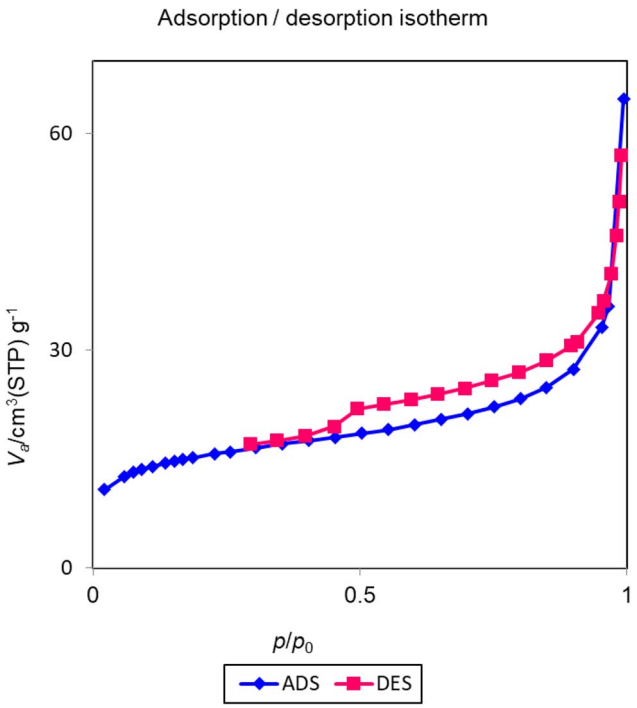

Fig. 5 N_2 adsorption–desorption isotherms of Cu-P.bis(OA)@FeB-MNPs.

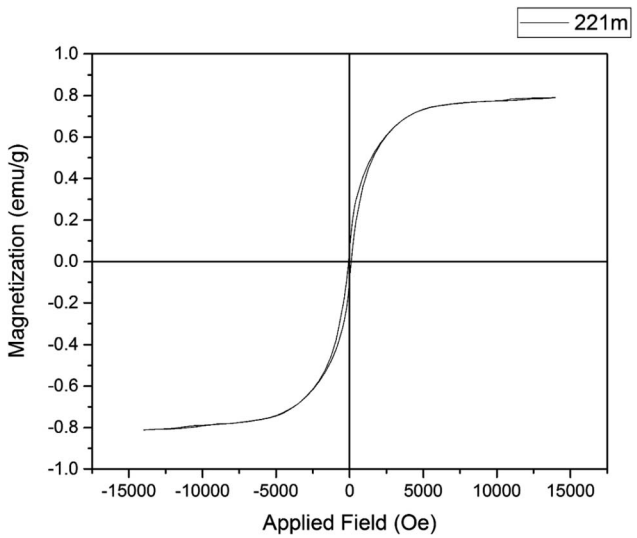

Fig. 6 Magnetization curves for Cu-P.bis(OA)@FeB-MNPs.

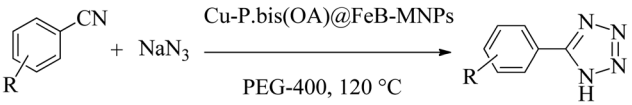

Scheme 5 The general progress for tetrazoles synthesis catalyzed by Cu-P.bis(OA)@FeB-MNPs.

composition of 3Cl-PTMS@FeB-MNPs shows the successful modification of FeB-MNPs with (3-chloropropyl)trimethoxysilane. The presence of N element in Cu-P.bis(OA)@FeB-MNPs confirmed that the P.bis(OA) ligand was successfully immobilized on the surface of FeB-MNPs. Also, the presence of Cu element confirmed that copper complex was successfully synthesized on the surface of the modified FeB-MNPs.

WDX analysis is another method for the qualitative study of the element content and their distribution in a sample. The WDX images of Cu-P.bis(OA)@FeB-MNPs are shown in Fig. 3. The WDX images confirmed the presence of C, N, O, Si, Fe, and Cu elements, which is in agreement with the obtained results

Table 1 Optimization of reaction conditions for the production of tetrazoles in the presence of Cu-P.bis(OA)@FeB-MNPs

Entry	Catalyst (mg)	Solvent	Temp. (°C)	Time (min)	Yield[a] (%)
1	—	PEG	120	720	NR
2	20	PEG	120	220	81
3	30	PEG	120	120	97
4	40	PEG	120	110	97
5	30	H_2O	Reflux	360	51
6	30	EtOH	Reflux	360	58
7	30	Dioxane	Reflux	360	53
8	30	DMSO	120	360	73
9	30	*n*-Hexane	Reflux	360	20
10	30	PEG	100	180	75

[a] The products were separated using thin layer chromatography.

Table 2 Synthesis of 5-substituted tetrazoles catalyzed by Cu-P.bis(OA)@FeB-MNPs

Entry	Nitrile	Product	Time (min)	Yield (%)	Melting point (°C)
1	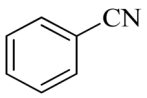	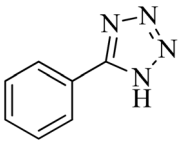	120	97	211–214 [ref. 14]
2	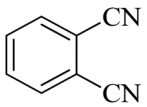	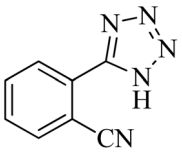	35	94	209–211 [ref. 53]
3	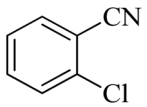	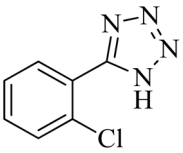	210	90	179–182 [ref. 37]
4	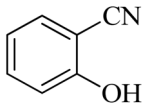	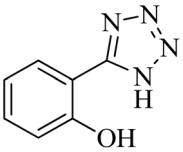	45	95	221–224 [ref. 54]
5	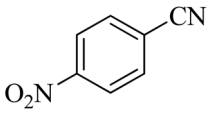	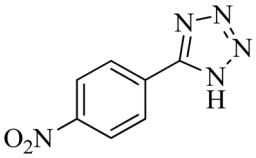	110	87	216–219 [ref. 55]
6	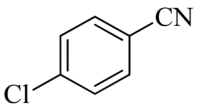	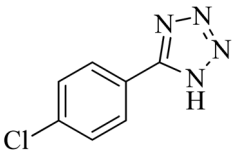	300	86	260–263 [ref. 56]
7	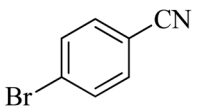	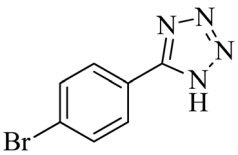	320	89	259–261 [ref. 14]
8	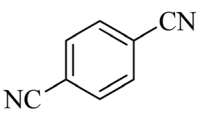	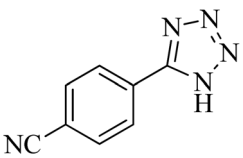	100	93	249–252 [ref. 55]
9	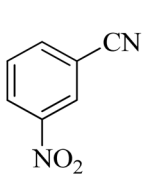	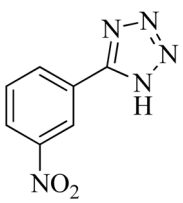	80	89	150–152 [ref. 37]

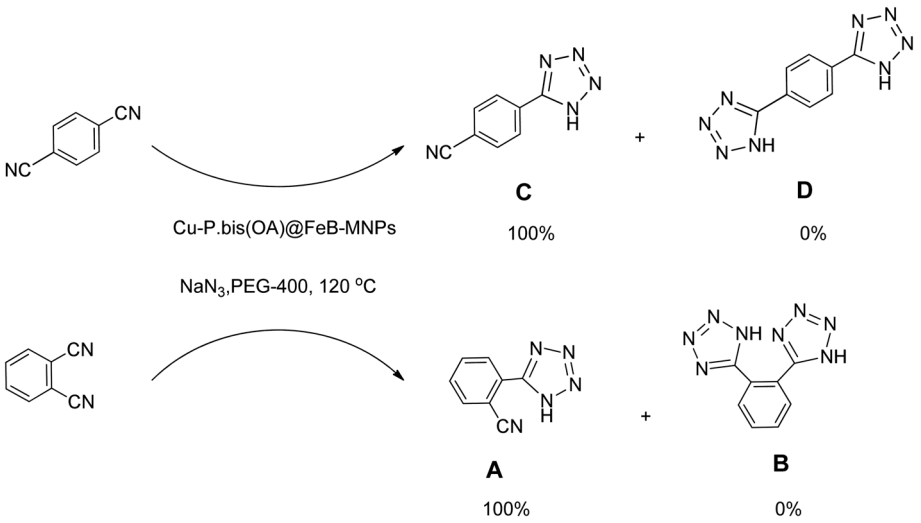

Scheme 6 Homoselectivity of Cu-P.bis(OA)@FeB-MNPs in the [3 + 2] cycloaddition of NaN_3 with terephthalonitrile and phthalonitrile.

from EDS analysis. In addition, the WDX images show a quite homogeneous distribution of C, N, O, Si, Fe, and Cu elements in the structure of Cu-P.bis(OA)@FeB-MNPs.

Because the copper element is the main catalytic active site of Cu-P.bis(OA)@FeB-MNPs, the exact concentration of Cu-metal was determined by AAS analysis, which was found to be 0.72×10^{-3} mol g^{-1}.

3.3. Studying the amount of organic ligand on FeB-MNPs using TGA

The content of Cl-PTMS and P.bis(OA) as organic layers that immobilized on FeB-MNPs was studied by TGA analysis. TGA and differential thermogravimetry (DTG) diagrams of Cu-P.bis(OA)@FeB-MNPs are outlined in Fig. 4. The TGA diagram of Cu-P.bis(OA)@FeB-MNPs indicated three steps of weight loss. The first of them is due to the evaporation of the absorbent solvents, which happened below 200 °C (about 3% of weight). It is very important that no weight loss happens up to 200 °C, except for the evaporation of the absorbent solvents, which means that Cu-P.bis(OA)@FeB-MNPs is stable and applicable up to 200 °C. The immobilized organic ligands on FeB-MNPs were decomposed after 200 °C, that indicated as the second step of weight loss in the TGA diagram. Therefore, P.bis(OA) ligand was successfully immobilized on the surface of FeB-MNPs. Finally, a small weight loss above 700 °C may be due to the continuation of biochar pyrolysis.

3.4. N_2 adsorption–desorption isotherms of Cu-P.bis(OA)@FeB-MNPs

The nitrogen adsorption/desorption technique is commonly used for the determination of the pore volume, pore diameter, and surface area of the materials. The resulting isotherms of nitrogen adsorption/desorption for Cu-P.bis(OA)@FeB-MNPs are investigated in Fig. 5. These isotherms display type H3 based on the IUPAC classification, which shows the pores structure of Cu-P.bis(OA)@FeB-MNPs.[52] Based on BET results, the specific surface area of Cu-P.bis(OA)@FeB-MNPs is 55.23 m^2 g^{-1}. Also, the total pore volume of Cu-P.bis(OA)@FeB-MNPs is 0.09 cm^3 g^{-1}, and the average pore diameter of Cu-P.bis(OA)@FeB-MNPs is 6.81 nm.

3.5. VSM curve of Cu-P.bis(OA)@FeB-MNPs

The magnetic property of Cu-P.bis(OA)@FeB-MNPs was studied with VSM by the "Magnetic Kavir Kashan" device, which is outlined in Fig. 6. As shown, Cu-P.bis(OA)@FeB-MNPs showed 0.8 emu g^{-1}, which is lower than the reported saturation magnetization for FeB-MNPs.[52] The decrease in the saturation magnetic property of Cu-P.bis(OA)@FeB-MNPs is due to the grafting of Cu-complex, P.bis(OA) ligand and silica layer on FeB-MNPs.

3.6. Catalytic performance of Cu-P.bis(OA)@FeB-MNPs in the synthesis of tetrazoles

The catalytic application of Cu-P.bis(OA)@FeB-MNPs was examined for the synthesis of tetrazoles. This catalyst showed a high efficiency and good selectivity in the cyclization reaction of [2 + 3] nitriles with sodium azide in the synthesis of tetrazoles (Scheme 5).

The catalytic performance of Cu-P.bis(OA)@FeB-MNPs is described in the homoselective production of nitrogen-rich heterocyclic 5-substituted tetrazoles *via* [3 + 2]cycloaddition reaction of NaN_3 with monofunctionalyzed benzonitriles. At first, the minimum required amount of Cu-P.bis(OA)@FeB-MNPs was checked in the [3 + 2]cycloaddition reaction of NaN_3 with unsubstituted benzonitrile (Ph–CN) for the formation of 5-phenyl-1*H*-tetrazole. No product was formed when zero amount of Cu-P.bis(OA)@FeB-MNPs was used (Table 1, entry 1). But, when the amount of Cu-P.bis(OA)@FeB-MNPs increases, the yield of synthesized 5-phenyl-1*H*-tetrazole product increases, and the reaction time decreases. Finally, the minimum required amount of Cu-P.bis(OA)@FeB-MNPs was optimized at 30 mg (Table 1, entry 3). Next, the effect of the solvent in the synthesis of 5-phenyl-1*H*-tetrazole was checked. Volatile solvents *e.g.* *n*-hexane, aprotic solvents *e.g.* DMSO and protic solvents were investigated in the production of 5-phenyl-1*H*-tetrazole using 30 mg of Cu-P.bis(OA)@FeB-MNPs to obtain

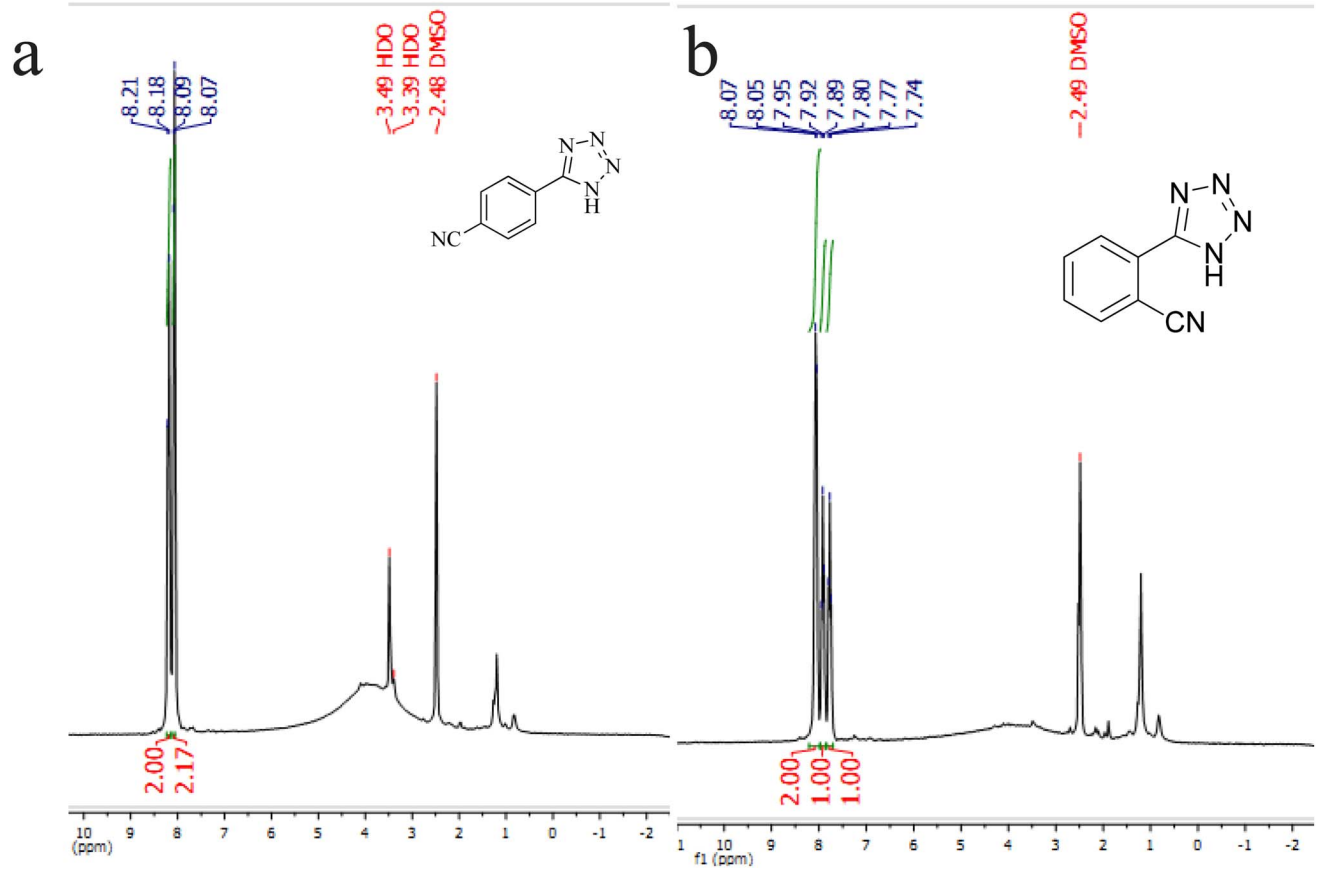

Fig. 7 ^{1}H NMR spectrum of 4-(1*H*-tetrazol-5-yl)benzonitrile (a) and 2-(1*H*-tetrazol-5-yl)benzonitrile (b).

the optimal conditions. As clearly shown in Table 1, the production of 5-phenyl-1*H*-tetrazole increased in polar solvents with high boiling point. Finally, the best results were obtained in the PEG-400 solvent. In addition, in the study of the effect of temperature, the best results were indicated at 120 °C. The model reaction was tested on a large scale of the reactants (NaN_3 (14 mmol, 0.9101 g) with benzonitriles (10 mmol, 1.0304 g)). The reaction yield was approximately 69% after 10 h.

In continuation, various 5-substituted tetrazole compounds were synthesized under the above-defined conditions in the presence of Cu-P.bis(OA)@FeB-MNPs as a catalyst. The details of the experimental results such as reaction time, efficiency, and TOF values are shown in Table 2. In which, the starting material of benzonitriles having an electron-donating or withdrawing groups on *meta*, *ortho*, or *para* position of the aromatic ring were tested and successfully converted to tetrazole products. As displayed in Table 2, the final 5-substituted tetrazoles were formed in excellent yields within a fast reaction rate in the presence of Cu-P.bis(OA)@FeB-MNPs.

Importantly, Cu-P.bis(OA)@FeB-MNPs exhibit homoselectivity in the formation of 5-substituted tetrazoles. Because, in the reaction of NaN_3 with dicyano-substituted benzonitriles (*e.g.* terephthalonitrile and phthalonitrile), only mono-addition happened in the presence of Cu-P.bis(OA)@FeB-MNPs (Scheme 6). These starting materials have two quite similar C≡N groups in their structure. The homoselectivity of Cu-P.bis(OA)@FeB-MNPs in the formation of 5-substituted tetrazoles through [3 + 2]cycloaddition of NaN_3 with terephthalonitrile and phthalonitrile were investigated using ^{1}H NMR. When phthalonitrile was used as the starting material, two products – 2-(1*H*-tetrazol-5-yl)benzonitrile (**A**) or 1,2-di(1*H*-tetrazol-5-yl) benzene (**B**) – were formed. As mentioned, one of the C≡N groups selectively reacted with NaN_3 for the synthesis of 2-(1*H*-

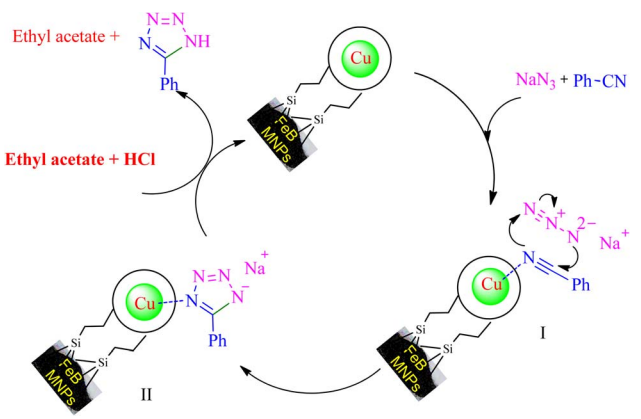

Scheme 7 The expected catalytic mechanism for the synthesis of 5-substituted tetrazoles using Cu-P.bis(OA)@FeB-MNPs.

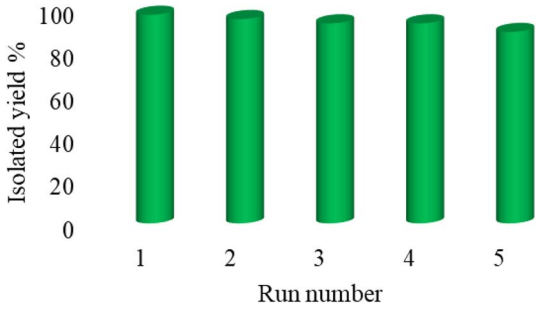

Fig. 8 The reusability of Cu-P.bis(OA)@FeB-MNPs.

tetrazol-5-yl)benzonitrile, and the other C≡N group did not react, and the 1,2-di(1*H*-tetrazol-5-yl)benzene product was not formed. As expected, when phthalonitrile was used, if product **A** was synthesized, more than two peaks should be observed in the ^{1}H NMR spectrum for aromatic hydrogens. But if **B** was synthesized, only two peaks should be observed in the ^{1}H NMR spectrum for aromatic hydrogens. As shown in the ^{1}H NMR spectrum of the final product from the [3 + 2] cycloaddition reaction of NaN_3 with phthalonitrile in the presence of Cu-P.bis(OA)@FeB-MNPs, three peaks were indicated for aromatic hydrogens (Fig. 7). Therefore, only product **A** was certainly formed, which indicates the homoselectively of Cu-P.bis(OA)@FeB-MNPs in the synthesis of tetrazoles.

When terephthalonitrile was used as the starting material, two products – 4-(1*H*-tetrazol-5-yl)benzonitrile (**C**) or 1,4-di(1*H*-tetrazol-5-yl)benzene (**D**) were formed. As mentioned, one of the C≡N groups selectively reacted with NaN_3 for the synthesis of **C**, the other C≡N group did not react, and the **D** product was not formed. As expected, when terephthalonitrile was used, if product **C** was synthesized, two peaks should have been observed in the ^{1}H NMR spectrum for aromatic hydrogens. But if **D** was synthesized, only one peak should have been observed in the ^{1}H NMR spectrum for aromatic hydrogens. As shown in the ^{1}H NMR spectrum of the final product from the [3 + 2] cycloaddition reaction of NaN_3 with terephthalonitrile in the presence of Cu-P.bis(OA)@FeB-MNPs, two peaks indicated the aromatic hydrogens (Fig. 7). Therefore, only product **C** was certainly formed, which indicates the homoselectively of Cu-P.bis(OA)@FeB-MNPs in the synthesis of tetrazoles.

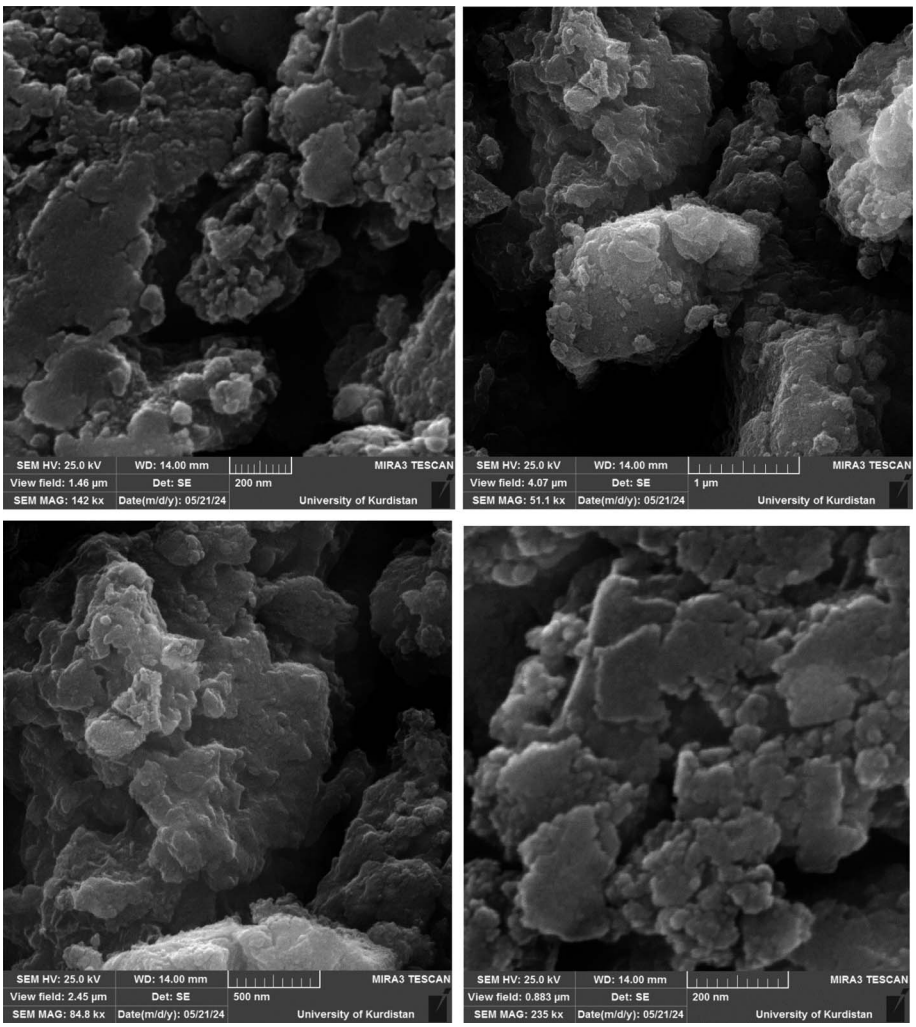

Fig. 9 SEM images of recycled Cu-P.bis(OA)@FeB-MNPs catalyst.

Based on the literature,[53,54,57] an expected mechanism is illustrated in Scheme 7 for the synthesizing of 5-substituted tetrazoles through [3 + 2] cycloaddition reaction of NaN_3 and nitriles in the presence of Cu-P.bis(OA)@FeB-MNPs. In this suggested mechanism, the interaction of the C≡N functional group with the active site of the catalyst causes the C≡N group to become susceptible to attack by azide ions, and the intermediate **II** is formed as sodium salt forms. The addition of HCl during workup converts the salt form of intermediate **II** to final tetrazole, which forms tetrazoles extracted in ethyl acetate.

3.7. Reusability of Cu-P.bis(OA)@FeB-MNPs

Practicability, reusability, stability, and availability are the determinative factors for catalysts. According to the emphasis of green chemistry on the reusability of catalysts, the reusability of Cu-P.bis(OA)@FeB-MNPs was investigated in the [3 + 2]cycloaddition reaction of NaN_3 with Ph–CN toward the formation of 5-phenyl-1*H*-tetrazole. In this regard, Cu-P.bis(OA)@FeB-MNPs were isolated after the completion of the reaction and then reused again without double activation. As indicated in Fig. 8, Cu-P.bis(OA)@FeB-MNPs can be recycled up to 6 times.

Also, the recycled Cu-P.bis(OA)@FeB-MNPs nanocatalyst was characterized by SEM (Fig. 9). The SEM images of recycled Cu-P.bis(OA)@FeB-MNPs catalyst showed that the morphology and size of this catalyst did not significantly change after reusing, therefore Cu-P.bis(OA)@FeB-MNPs catalyst was stable after reusing.

3.8. Comparison of Cu-P.bis(OA)@FeB-MNPs with other catalysts

The practicability of Cu-P.bis(OA)@FeB-MNPs was compared with other reported catalysts (Table 3). The [3 + 2] cycloaddition reaction of NaN_3 and Ph–CN in the presence of Cu-P.bis(OA)@FeB-MNPs was compared with other catalysts. As indicated, Cu-P.bis(OA)@FeB-MNPs exhibit 98% of the product within only 2 h, which indicates a better yield and reaction time than the other catalysts. Besides, several reports in literature formed from unrenewable materials or used hazard solvents or limited by time-consuming or difficult catalyst recovery. While FeB-MNPs are formed from renewable materials as an ideal waste recycling and Cu-P.bis(OA)@FeB-MNPs can easily be recovered and reused. More addition, 5-substituted tetrazoles were synthesized in the green solvent (PEG-400) in the presence of Cu-P.bis(OA)@FeB-MNPs.

Table 3 Comparison results of Cu-P.bis(OA)@FeB-MNPs with other catalysts in the formation of 5-phenyl-1*H*-tetrazole

Entry	Catalyst	Time (h)	Yield (%)	Ref.
1	CoY zeolite	14	90	58
2	Cu–Zn alloy nanopowder	10	95	59
3	$B(C_6F_5)_3$	8	94	60
4	Fe_3O_4@SiO_2/salen Cu(II)	7	90	61
5	Fe_3O_4/ZnS HNSs	24	81.1	62
6	Mesoporous ZnS	36	86	63
7	$AgNO_3$	5	83	64
8	$CuFe_2O_4$	12	82	65
9	Nano ZnO/Co_3O_4	12	90	66
10	Ni-MP(AMP)$_2$@Fe-biochar	3.8	92	52
12	Fe_3O_4@boehmite NPs	4	97	67
13	Cu(II)[Sal(PMeOSi)DETA]@KIT-6	3	94	68
14	KIT-6@DABP@Cu	5	91	69
15	KIT-6@SMTU@Ni	3	95	70
16	Cu-TDBB@MCM-41/Fe_3O_4	7	90	71
17	Nd-Schiff-base@BMNPs	3	98	48
18	Nd-bis(PYT)@boehmite NPs	2.5	97	53
19	Pd–SMTU@boehmite	2.5	95	72
20	Cu-P.bis(OA)@FeB-MNPs	2	97	This work

4. Conclusions

In this work, magnetic biochar NPs (FeB-MNPs) were synthesized *via* pyrolysis of chicken manure, which is a new process for recycling waste. Then, the performed biochar was magnetized by magnetic Fe(0) nanoparticles to improve its recovery. Then, a new copper complex was immobilized on its surface and used as a selective, inexpensive, stable, recoverable, practicable, and available catalyst for the synthesis of 5-substituted tetrazoles. This catalyst (Cu-P.bis(OA)@FeB-MNPs) was characterized by WDX, SEM, TGA, EDS, VSM, AAS, and N_2 adsorption–desorption (BET method) techniques. SEM images indicated that the particles of this catalyst are less than 70 nm in size. TGA analysis confirmed that the P.bis(OA) ligand was successfully supported on FeB-MNPs and Cu-P.bis(OA)@FeB-MNPs is stable up to 200 °C. EDS and WDX confirmed that the surface of FeB-MNPs was successfully modified by Cl-PTMS and then functionalized by the P.bis(OA) ligand and the copper complex was formed on the surface of functionalized FeB-MNPs. VSM analysis indicated that this catalyst can be recovered by an external magnet. Therefore, it was recovered and reused for several runs. The BET method showed good surface area for Cu-P.bis(OA)@FeB-MNPs, therefore, this catalyst has high efficiency and activity in the synthesis of 5-substituted tetrazoles.

Author contributions

Marwan Majeed Maseer: methodology. Tavan Kikhavani: supervision, project administration, formal analysis. Bahman Tahmasbi: supervision, conceptualization, formal analysis, resources, project administration, writing – original draft, writing review and editing.

Conflicts of interest

The authors declare no conflict of interest and competing interests.

Acknowledgements

The authors thank the research facilities of Ilam University, Ilam, Iran, for financial support of this research project.

References

1 S. L. Tang, R. L. Smith and M. Poliakoff, Principles of green chemistry: productively, *Green Chem.*, 2005, **7**, 761–762.
2 P. T. Anastas and J. C. Warner, Principles of green chemistry, *Green Chemistry: Theory and Practice*, 1998, vol. 29, pp. 14821–14842.
3 V. Ahluwalia, M. Kidwai, V. Ahluwalia and M. Kidwai, Basic principles of green chemistry, *New trends in green chemistry*, 2004, pp. 5–14.
4 P. Anastas and N. Eghbali, Green chemistry: principles and practice, *Chem. Soc. Rev.*, 2010, **39**, 301–312.
5 W. Abdussalam-Mohammed, A. Q. Ali and A. Errayes, Green chemistry: principles, applications, and disadvantages, *Chem. Methodol.*, 2020, **4**, 408–423.
6 D. Astruc, F. Lu and J. R. Aranzaes, Nanoparticles as recyclable catalysts: the frontier between homogeneous and heterogeneous catalysis, *Angew. Chem., Int. Ed. Engl.*, 2005, **44**, 7852–7872.
7 A. Corma and H. Garcia, Crossing the borders between homogeneous and heterogeneous catalysis: developing recoverable and reusable catalytic systems, *Top. Catal.*, 2008, **48**, 8–31.
8 F. Poovan, V. G. Chandrashekhar, K. Natte and R. V. Jagadeesh, Synergy between homogeneous and heterogeneous catalysis, *Catal. Sci. Technol.*, 2022, **12**, 6623–6649.
9 S. Shylesh, V. Schünemann and W. R. Thiel, Magnetically separable nanocatalysts: bridges between homogeneous and heterogeneous catalysis, *Angew. Chem., Int. Ed. Engl.*, 2010, **49**, 3428–3459.
10 V. Polshettiwar and R. S. Varma, Green chemistry by nano-catalysis, *Green Chem.*, 2010, **12**, 743–754.
11 S. B. Somwanshi, S. B. Somvanshi and P. B. Kharat, Nanocatalyst: A Brief Review on Synthesis to Applications, *J. Phys.: Conf. Ser.*, 2020, 012046.
12 P. Saini, S. Meena, D. K. Mahawar, A. Dandia and V. Parewa, Principles and Concepts of Nanocatalysis, *Advanced Nanocatalysis for Organic Synthesis and Electroanalysis*, 2022, p. 1.
13 B. Tahmasbi, M. Darabi and M. Nikoorazm, A new Schiff-base complex of palladium nanoparticles on modified boehmite with di(pyridin-2-yl)methanone as a robust, reusable, and selective nanocatalyst in the C–C coupling reaction, *Appl. Organomet. Chem.*, 2024, **38**, e7348.
14 P. Moradi, T. Kikhavani and Y. Abbasi Tyula, A new samarium complex of 1,3-bis(pyridin-3-ylmethyl)thiourea on boehmite nanoparticles as a practical and recyclable nanocatalyst for the selective synthesis of tetrazoles, *Sci. Rep.*, 2023, **13**, 5902.
15 A. Jabbari, P. Moradi, M. Hajjami and B. Tahmasbi, Tetradentate copper complex supported on boehmite nanoparticles as an efficient and heterogeneous reusable nanocatalyst for the synthesis of diaryl ethers, *Sci. Rep.*, 2022, **12**, 11660.
16 A. Jabbari, M. Nikoorazm and P. Moradi, Two Schiff-base complexes of cadmium and manganese on modified MCM-41 as practical, recyclable and selective nanocatalysts for the synthesis of sulfoxides, *J. Porous Mater.*, 2023, **30**, 1395–1402.
17 A. Jabbari, M. Nikoorazm and P. Moradi, AV (O)-Schiff-base complex on MCM-41 as an efficient, reusable, and chemoselective nanocatalyst for the oxidative coupling of thiols and oxidation of sulfides, *Res. Chem. Intermed.*, 2023, **49**, 1485–1505.
18 R. S. Salama, S. M. El-Bahy and M. A. Mannaa, Sulfamic acid supported on mesoporous MCM-41 as a novel, efficient and reusable heterogenous solid acid catalyst for synthesis of xanthene, dihydropyrimidinone and coumarin derivatives, *Colloids Surf., A*, 2021, **628**, 127261.
19 P. Moradi and M. Hajjami, Magnetization of graphene oxide nanosheets using nickel magnetic nanoparticles as a novel support for the fabrication of copper as a practical, selective, and reusable nanocatalyst in C–C and C–O coupling reactions, *RSC Adv.*, 2021, **11**, 25867–25879.
20 H. M. Altass, M. Morad, A. E.-R. S. Khder, M. A. Mannaa, R. S. Jassas, A. A. Alsimaree, *et al.*, Enhanced catalytic activity for CO oxidation by highly active Pd nanoparticles supported on reduced graphene oxide/copper metal organic framework, *J. Taiwan Inst. Chem. Eng.*, 2021, **128**, 194–208.
21 H. M. Altass, S. A. Ahmed, R. S. Salama, Z. Moussa, R. S. Jassas, R. I. Alsantali, *et al.*, Low temperature CO oxidation over highly active gold nanoparticles supported on reduced graphene oxide@Mg-BTC nanocomposite, *Catal. Lett.*, 2023, **153**, 876–886.
22 A. Rezaei, A. Ghorbani-Choghamarani and B. Tahmasbi, Synthesis and characterization of nickel metal-organic framework including 4,6-diamino-2-mercaptopyrimidine and its catalytic application in organic reactions, *Catal. Lett.*, 2023, **153**, 2005–2017.
23 S. A. El-Hakam, S. E. Samra, S. M. El-Dafrawy, A. A. Ibrahim, R. S. Salama and A. I. Ahmed, Synthesis of sulfamic acid supported on Cr-MIL-101 as a heterogeneous acid catalyst and efficient adsorbent for methyl orange dye, *RSC Adv.*, 2018, **8**, 20517–20533.
24 R. S. Salama, S. El-Hakam, S. Samra, S. El-Dafrawy and A. Ahmed, Cu-BDC as a Novel and Efficient Catalyst for the Synthesis of 3,4-Dihydropyrimidin-2(1*H*)-ones and Aryl-14*H*-dibenzo[*a*,*j*]Xanthenes under Conventional Heating, *Int. J. Nano Mater. Sci.*, 2018, **7**, 31–42.
25 R. S. Salama, S. El-Hakam, S. Samra, S. El-Dafrawy and A. Ahmed, Adsorption, equilibrium and kinetic studies on the removal of methyl orange dye from aqueous solution by using of copper metal organic framework (Cu-BDC), *Int. J. Mod. Chem.*, 2018, **10**, 195–207.
26 S. M. El-Dafrawy, R. S. Salama, S. A. El-Hakam and S. E. Samra, Bimetal-organic frameworks (Cu_x–Cr_{100-x}–MOF) as a stable and efficient catalyst for synthesis of 3,4-dihydropyrimidin-2-one and 14-phenyl-14*H*-dibenzo[*a*,*j*] xanthene, *J. Mater. Res. Technol.*, 2020, **9**, 1998–2008.

27 R. S. Salama, A. El-Hakam, S. Samra, S. El-Dafrawy, A. A. Ibrahim and A. I. Ahmed, Removal of methyl orange (MO) from aqueous solution by bimetal-organic frameworks (Cu_x–Cr_{100-x}–MOF): kinetics and isotherms studies, *Delta University Scientific Journal*, 2023, **6**, 266–277.
28 R. S. Salama, S. M. Hassan, A. I. Ahmed, W. A. El-Yazeed and M. A. Mannaa, The role of PMA in enhancing the surface acidity and catalytic activity of a bimetallic Cr–Mg-MOF and its applications for synthesis of coumarin and dihydropyrimidinone derivatives, *RSC Adv.*, 2020, **10**, 21115–21128.
29 R. S. Salama, M. A. Mannaa, H. M. Altass, A. A. Ibrahim and A. E.-R. S. Khder, Palladium supported on mixed-metal–organic framework (Co–Mn-MOF-74) for efficient catalytic oxidation of CO, *RSC Adv.*, 2021, **11**, 4318–4326.
30 R. Salama, Synthesis, characterization and catalytic activities of sulfuric acid loaded on copper metal organic frameworks (Cu-BDC), *Delta University Scientific Journal*, 2019, **2**, 10–15.
31 F. T. Alshorifi, D. E. Tobbala, S. M. El-Bahy, M. A. Nassan and R. S. Salama, The role of phosphotungstic acid in enhancing the catalytic performance of UiO-66 (Zr) and its applications as an efficient solid acid catalyst for coumarins and dihydropyrimidinones synthesis, *Catal. Commun.*, 2022, **169**, 106479.
32 Y. Zhai, Z. Zhu and S. Dong, Carbon-based nanostructures for advanced catalysis, *ChemCatChem*, 2015, **7**, 2806–2815.
33 P. Wang, Q. Dong, C. Gao, W. Bai, D. Chu and Y. He, A comprehensive review of carbon nanotubes: growth mechanisms, preparation and applications, *Fullerenes, Nanotubes Carbon Nanostruct.*, 2024, **32**, 415–429.
34 H. Matsumoto, T. Iwai, M. Sawamura and Y. Miura, Continuous-Flow Catalysis Using Phosphine-Metal Complexes on Porous Polymers: Designing Ligands, Pores, and Reactors, *ChemPlusChem*, 2024, e202400039.
35 S. Jaiswal, J. Dwivedi, D. Kishore and S. Sharma, Green Methodologies for Tetrazole Synthesis from Different Starting Materials: A Recent Update, *Curr. Org. Chem.*, 2024, **28**, 134–160.
36 M. Norouzi and P. Moradi, A new copper complex on functionalized magnetic biochar nano-sized materials as sustainable heterogeneous catalysts for C–O bond formation in the natural deep eutectic solvent, *Biomass Convers. Biorefin.*, 2023, 1–13, DOI: **10.1007/s13399-023-05163-z**.
37 P. Moradi, B. Zarei, Y. Abbasi Tyula and M. Nikoorazm, Novel neodymium complex on MCM-41 magnetic nanocomposite as a practical, selective, and returnable nanocatalyst in the synthesis of tetrazoles with antifungal properties in agricultural, *Appl. Organomet. Chem.*, 2023, **37**, e7020.
38 M. Alekasir, S. Heydarian and B. Tahmasbi, The synthesis of biochar from biomass waste recycling and its surface modification for immobilization of a new Cu complex as a reusable nanocatalyst in the homoselective synthesis of tetrazoles, *Res. Chem. Intermed.*, 2024, **50**, 2031–2049.
39 S.-Z. Zhang, Z.-S. Cui, M. Zhang and Z.-H. Zhang, Biochar-based functional materials as heterogeneous catalysts for organic reactions, *Curr. Opin. Green Sustainable Chem.*, 2022, **38**, 100713.
40 L.-N. Dong, S.-Z. Zhang, W.-L. Zhang, Y. Dong, L.-P. Mo and Z.-H. Zhang, Synthesis, characterization and application of magnetic biochar sulfonic acid as a highly efficient recyclable catalyst for preparation of spiro-pyrazolo[3,4-*b*] pyridines, *Res. Chem. Intermed.*, 2022, **48**, 1249–1272.
41 A. Ivanković, A. Dronjić, A. M. Bevanda and S. Talić, Review of 12 principles of green chemistry in practice, *Int. J. Sustainable Green Energy*, 2017, **6**, 39–48.
42 R. A. Sheldon, Fundamentals of green chemistry: efficiency in reaction design, *Chem. Soc. Rev.*, 2012, **41**, 1437–1451.
43 K. Weber and P. Quicker, Properties of biochar, *Fuel*, 2018, **217**, 240–261.
44 J. Lee, K.-H. Kim and E. E. Kwon, Biochar as a catalyst, *Renewable Sustainable Energy Rev.*, 2017, **77**, 70–79.
45 X. Cao, S. Sun and R. Sun, Application of biochar-based catalysts in biomass upgrading: a review, *RSC Adv.*, 2017, **7**, 48793–48805.
46 R. Shan, J. Han, J. Gu, H. Yuan, B. Luo and Y. Chen, A review of recent developments in catalytic applications of biochar-based materials, *Resour., Conserv. Recycl.*, 2020, **162**, 105036.
47 H. Lyu, Q. Zhang and B. Shen, Application of biochar and its composites in catalysis, *Chemosphere*, 2020, **240**, 124842.
48 B. Tahmasbi, P. Moradi and M. Darabi, A new neodymium complex on renewable magnetic biochar nanoparticles as an environmentally friendly, recyclable and efficient nanocatalyst in the homoselective synthesis of tetrazoles, *Nanoscale Adv.*, 2024, **6**, 1932–1944.
49 M.-N. Chen, L.-P. Mo, Z.-S. Cui and Z.-H. Zhang, Magnetic nanocatalysts: synthesis and application in multicomponent reactions, *Curr. Opin. Green Sustainable Chem.*, 2019, **15**, 27–37.
50 S. Z. Zhang, L. N. Dong, L. P. Mo and Z. H. Zhang, Magnetic biochar-supported ZrO_2 as an efficient catalyst for one-pot synthesis of 1′, 4′-dihydro-3*H*,3′*H*-spiro[furo[3,4-*b*] quinoline-9,2′-quinoxaline]-1,3′(4*H*)-diones, *Appl. Organomet. Chem.*, 2023, **37**, e6949.
51 L. N. Dong, Y. M. Wang, W. L. Zhang, L. P. Mo and Z. H. Zhang, Nickel supported on magnetic biochar as a highly efficient and recyclable heterogeneous catalyst for the one-pot synthesis of spirooxindole-dihydropyridines, *Appl. Organomet. Chem.*, 2022, **36**, e6667.
52 P. Moradi and M. Hajjami, Magnetization of biochar nanoparticles as a novel support for fabrication of organo nickel as a selective, reusable and magnetic nanocatalyst in organic reactions, *New J. Chem.*, 2021, **45**, 2981–2994.
53 Y. Abbasi Tyula, P. Moradi and M. Nikoorazm, A New Neodymium Complex on Boehmite Nanoparticles with 1,3-Bis(pyridine-3-ylmethyl)thiourea as a Practical and Reusable Nanocatalyst for the Chemoselective Synthesis of Tetrazoles, *ChemistrySelect*, 2023, **8**, e202301674.
54 A. Jabbari, P. Moradi and B. Tahmasbi, Synthesis of tetrazoles catalyzed by a new and recoverable nanocatalyst of cobalt on modified boehmite NPs with 1,3-bis(pyridin-3-ylmethyl)thiourea, *RSC Adv.*, 2023, **13**, 8890–8900.

55 M. Akbari, M. Nikoorazm, B. Tahmasbi and A. Ghorbani-Choghamarani, Homoselective synthesis of tetrazoles and chemoselective oxidation of sulfides using Ni(II)-Schiff base complex stabilized on 3-dimensional mesoporous KIT-6 surface as a recyclable nanocatalyst, *Inorg. Chem. Commun.*, 2024, **160**, 111852.

56 B. Tahmasbi, M. Nikoorazm, P. Moradi and Y. A. Tyula, A Schiff base complex of lanthanum on modified MCM-41 as a reusable nanocatalyst in the homoselective synthesis of 5-substituted 1*H*-tetrazoles, *RSC Adv.*, 2022, **12**, 34303–34317.

57 B. Tahmasbi, M. Nikoorazm, P. Moradi and Y. Abbasi Tyula, A Schiff base complex of lanthanum on modified MCM-41 as a reusable nanocatalyst in the homoselective synthesis of 5-substituted 1*H*-tetrazoles, *RSC Adv.*, 2022, **12**, 34303–34317.

58 V. Rama, K. Kanagaraj and K. Pitchumani, Syntheses of 5-substituted 1*H*-tetrazoles catalyzed by reusable CoY zeolite, *J. Org. Chem.*, 2011, **76**, 9090–9095.

59 G. Aridoss and K. K. Laali, Highly efficient synthesis of 5-substituted 1*H*-tetrazoles catalyzed by Cu–Zn alloy nanopowder, conversion into 1,5-and 2,5-disubstituted tetrazoles, and synthesis and NMR studies of new tetrazolium ionic liquids, *Eur. J. Org Chem.*, 2011, **2011**, 6343–6355.

60 S. K. Prajapti, A. Nagarsenkar and B. N. Babu, An efficient synthesis of 5-substituted 1*H*-tetrazoles *via* B $(C_6F_5)_3$ catalyzed [3 + 2] cycloaddition of nitriles and sodium azide, *Tetrahedron Lett.*, 2014, **55**, 3507–3510.

61 F. Dehghani, A. R. Sardarian and M. Esmaeilpour, Salen complex of Cu (II) supported on superparamagnetic Fe_3O_4@SiO_2 nanoparticles: an efficient and recyclable catalyst for synthesis of 1-and 5-substituted 1*H*-tetrazoles, *J. Organomet. Chem.*, 2013, **743**, 87–96.

62 G. Qi, W. Liu and Z. Bei, Fe_3O_4/ZnS Hollow Nanospheres: A Highly Efficient Magnetic Heterogeneous Catalyst for Synthesis of 5-Substituted 1*H*-Tetrazoles from Nitriles and Sodium Azide, *Chin. J. Chem.*, 2011, **29**, 131–134.

63 L. Lang, H. Zhou, M. Xue, X. Wang and Z. Xu, Mesoporous ZnS hollow spheres-catalyzed synthesis of 5-substituted 1*H*-tetrazoles, *Mater. Lett.*, 2013, **106**, 443–446.

64 P. Mani, A. K. Singh and S. K. Awasthi, $AgNO_3$ catalyzed synthesis of 5-substituted-1*H*-tetrazole *via* [3 + 2] cycloaddition of nitriles and sodium azide, *Tetrahedron Lett.*, 2014, **55**, 1879–1882.

65 B. Sreedhar, A. S. Kumar and D. Yada, $CuFe_2O_4$ nanoparticles: a magnetically recoverable and reusable catalyst for the synthesis of 5-substituted 1*H*-tetrazoles, *Tetrahedron Lett.*, 2011, **52**, 3565–3569.

66 S. M. Agawane and J. M. Nagarkar, Synthesis of 5-substituted 1*H*-tetrazoles using a nano ZnO/Co_3O_4 catalyst, *Catal. Sci. Technol.*, 2012, **2**, 1324–1327.

67 P. Moradi, Investigation of Fe_3O_4@boehmite NPs as efficient and magnetically recoverable nanocatalyst in the homoselective synthesis of tetrazoles, *RSC Adv.*, 2022, **12**, 33459–33468.

68 M. Akbari, M. Nikoorazm, B. Tahmasbi and A. Ghorbani-Choghamarani, The new Schiff-base complex of copper (II) grafted on mesoporous KIT-6 as an effective nanostructure catalyst for the homoselective synthesis of various tetrazoles, *Appl. Organomet. Chem.*, 2024, **38**, e7317.

69 M. Darabi, M. Nikoorazm, B. Tahmasbi and A. Ghorbani-Choghamarani, Homoselective synthesis of tetrazole derivatives using copper complex anchored on mesoporous KIT-6 as a reusable, highly efficient, and environmentally green nanocatalyst, *Appl. Organomet. Chem.*, 2024, **38**, e7392.

70 M. Darabi, M. Nikoorazm, B. Tahmasbi and A. Ghorbani-Choghamarani, Immobilization of Ni (ii) complex on the surface of mesoporous modified-KIT-6 as a new, reusable and highly efficient nanocatalyst for the synthesis of tetrazole and pyranopyrazole derivatives, *RSC Adv.*, 2023, **13**, 12572–12588.

71 M. Nikoorazm, B. Tahmasbi, S. Gholami, M. Khanmoradi, Y. A. Tyula, M. Darabi, *et al.*, Synthesis and characterization of a new Schiff-base complex of copper on magnetic MCM-41 nanoparticles as efficient and reusable nanocatalyst in the synthesis of tetrazoles, *Polyhedron*, 2023, **244**, 116587.

72 P. Moradi and A. Ghorbani-Choghamarani, Efficient synthesis of 5-substituted tetrazoles catalysed by palladium–*S*-methylisothiourea complex supported on boehmite nanoparticles, *Appl. Organomet. Chem.*, 2017, **31**, e3602.